Effect of Through-Bond Interaction on Conformation and Structure in Rod-Shaped Donor–Acceptor Systems

Part 2

Crystal Structures of Seven *N*-Aryltropan-3-one (= 8-Aryl-8-azabicyclo[3.2.1]octan-3-one) Derivatives

by **Dirk J. A. De Ridder***, **Kees Goubitz**, and **Henk Schenk**

Laboratory for Crystallography, Institute of Molecular Chemistry, Faculty of Science, University of Amsterdam, Nieuwe Achtergracht 166, NL-1018 WV Amsterdam
(phone: (31)-20-5257039; fax: (31)-20-5256940; e-mail: dirkdr@science.uva.nl)

and

Bert Krijnen[1]) and **Jan W. Verhoeven**

Laboratory of Organic Chemistry, Institute of Molecular Chemistry, Faculty of Science, University of Amsterdam, Nieuwe Achtergracht 129, NL-1018 WS Amsterdam

The crystal structures of seven *N*-aryltropan-3-one (= 8-aryl-8-azabicyclo[3.2.1]octan-3-one) derivatives **1T1**, **2T1**, **2T2**, **3T2**, **5T2**, **2T3**, and **3T3** are presented (*Fig. 2* and *Tables 1–5*) and discussed together with the derivatives **1T2** and **4T2** published previously. The piperidine ring adopts a chair conformation. In all structures, the aryl group is in the axial position, with the plane through the aryl C-atoms nearly perpendicular to the mirror plane of the piperidine ring. The through-bond interaction between the piperidine ring N-atom (one-electron donor) and the substituted exocyclic C=C bond (acceptor) not only elongates the central C–C bonds of the piperidine ring but also increases the pyrimidalization at C(4) of the piperidine ring. Flattening of the C(2)–C(6) part of the piperidine ring decreases the through-bond interaction.

1. Introduction. – In 1968, the term through-bond interaction (TBI) was introduced by *Hoffmann et al.* [1] to designate the intramolecular interaction between functional groups *via* connecting σ-bonds. According to this concept, the orbitals of the functional groups may interact with each other as a consequence of their mutual mixing with the intervening σ-bonds.

Krijnen [2] investigated systematically whether TBI donor–acceptor interactions can be found in the donor–acceptor compounds shown in *Fig. 1*. Both these systems contain a substituted N-atom as the potential one-electron donor and a substituted exocyclic C=C bond as the potential acceptor, whereas donor and acceptor are separated by three σ-bonds in a well-defined arrangement.

In the first part of this series of three papers, the crystal structures of seven *N*-arylpiperidin-4-one derivatives **nPm** were presented and discussed [3]. In all compounds, the piperidine ring adopts a normal chair conformation. In all but one structure, **1P2**, the aryl group attached at the piperidine N-atom was found in the

[1]) Permanent address: *Unilever R & D Vlaardingen*, Olivier van Noortlaan 120, NL-3133 AT Vlaardingen.

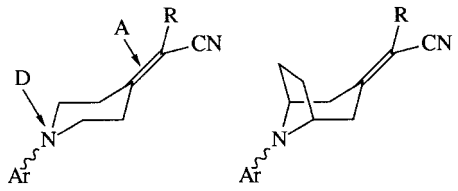

Fig. 1. *Donor–acceptor compounds investigated. Left:* piperidin-4-one-like systems [3], *right:* tropanone-like systems (this paper). D = Donor, A = Acceptor; R = CN, MeOCO; Ar = Ph, 4-Me–C_6H_4, 3,5-Me_2–C_6H_3, 4-MeO–C_6H_4, 4-F–C_6H_4, 2,4,6-Me_3–C_6H_2.

equatorial position. In this axial structure **1P2**, the piperidine ring central C–C bond was significantly elongated compared to the equatorial **nPm** derivatives. It was also observed that TBI is influencing the pyramidalization at C(4) of piperidine, in such a way that a strong interaction is directing the ethylene C-atom C(9) in the axial direction.

In this contribution, the crystal structures of seven *N*-aryltropan-3-one (= 8-aryl-8-azabicyclo[3.2.1]octan-3-one) derivatives will be discussed together with those of two *N*-aryltropan-3-one derivatives already published [4]. This will enable the investigation of the influence of the additional $-CH_2-CH_2-$ bridge on the parameters discussed previously [3].

2. Results and Discussion. – The systematic code (*Scheme*) introduced by *Krijnen* [2] to indicate the compounds studied will also be used here; it was briefly summarized in the first part of this series [3].

X-Ray crystal structures have been determined for the compounds **1T1**, **2T1**, **1T2**–**5T2**, **2T3**, and **3T3**; *Krijnen et al.* [4] already reported the synthesis and X-ray structures of **1T2** and **4T2**. Attempts to determine the X-ray structure of **3T1** were unsuccessful. Crystallographic data are given in *Table 1*, and selected bond lengths and angles are compiled in *Table 2*. In *Fig. 2*, ORTEP drawings of the X-ray structures are presented together with an arbitrary atom-numbering system.

2.1. *Orientation of the* N-*Aryl Group*. In the **nTm** structures, the aryl group is invariably found in the axial orientation (*Fig. 2*), which may seem to be unsurprising since steric hindrance between this group and the *exo*-H-atoms of the $-CH_2CH_2-$ bridge disfavors the equatorial conformation. The exclusively axial orientation of the *N*-substituent found in the X-ray structures of the **nTm** derivatives is not a 'normal' structural feature of the solid-state structure of tropane-like systems. A search in the April 2002 release of the *Cambridge Structural Database* (*CSD*) [5] on a tropane-like system yielded 60 X-ray structures with one non-H-substituent on the N-atom. With the exception of VATZUL (**1T2**) and VAVBAV (**4T2**), the C(4)-atom is saturated in all cases. In 30 of these X-ray structures, the N-atom is protonated, with the H-atom always occupying the axial position. In the unprotonated derivatives, however, the *N*-substituent is found either in the equatorial or the axial position. In three of these unprotonated derivatives, a *N*-aryl substituent is present in the axial position: VATZUL (**1T2**) and VAVBAV (**4T2**) determined by *Krijnen et al.* [4], and DUZHEL [6] that has, like **4T2**, a 4-methoxyphenyl substituent. Furthermore, it is generally

Scheme. *Explanation of the Codes Used to Indicate the Compounds Studied*. At the bottom, the reaction scheme of the *Knoevenagel*-type condensation [24] is shown.

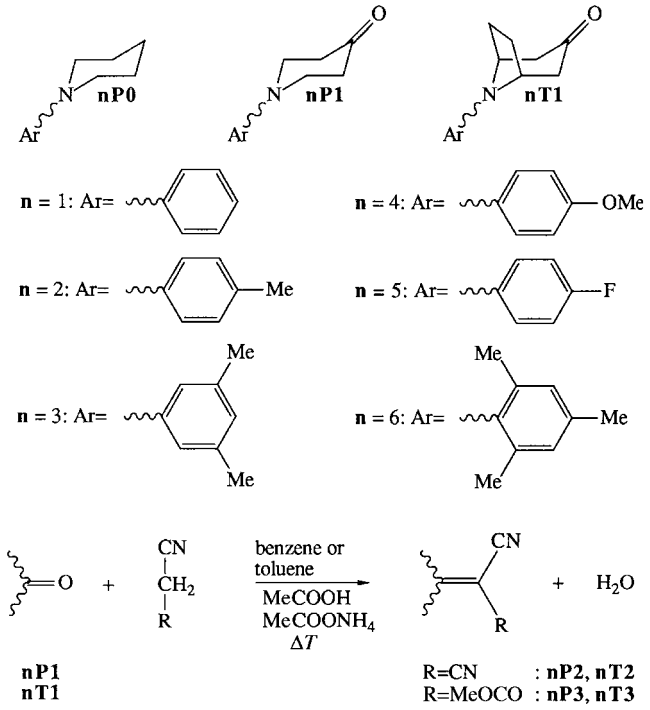

accepted that, in solution, both the axial and equatorial conformations of these tropane-like systems may be populated to an appreciable extent [7–9].

The fact that, in the available X-ray structures of **nTm**, the *N*-aryl group is exclusively found in the axial orientation is, therefore, a strong indication that this axial conformation of the donor–acceptor systems is thermodynamically the most stable one in solution, *i.e.*, the small energetic stabilization of the axial conformer of **nTm** offered by TBI in such a conformer results in a pronounced preference for this conformation.

2.2. N-*Aryltropan-3-ones.* Compounds **1T1** and **2T1** differ by only a Me group on the aryl ring in the position *para* to the C-atom attached to the N-atom. From a crystallographic viewpoint, these structures are closely related (*cf. Table 1* and *Fig. 3*). In both cases, a final difference *Fourier* map revealed a substantial residual electron density that is undoubtedly attributable to one of the solvents used to (re)crystallize the compounds (*cf. Fig. 3*). Unfortunately, no unambiguous explanation could be given, and, combined with the crystals being of rather poor quality, the structural data retrieved were not very precise (*cf.* high e.s.d.'s in *Table 2*).

2.3. *Configuration of the Piperidine Ring.* The strength of TBI is thought to be sensitive to the orientation of the interacting donor and acceptor orbitals with respect to the σ-relay connecting them, and also [1][10] for the conformation of the σ-relay itself. Therefore, the conformation of the central piperidine ring should be examined

Table 1. *Crystallographic Data of* N-*Aryltropanones* **1T1**, **2T1**, **2T2**, **3T2**, **5T2**, **2T3**, *and* **3T3**. For the methods used in the structure determination, see *Exper. Part*. The crystallographic data of **1T2** and **4T2** have been published in [4].

	1T1	**2T1**	**2T2**	**3T2**	**5T2**	**2T3**	**3T3**
Formula	$C_{13}H_{15}NO$	$C_{14}H_{17}NO$	$C_{17}H_{17}N_3$	$C_{18}H_{19}N_3$	$C_{16}H_{14}FN_3$	$C_{18}H_{20}N_2O_2$	$C_{19}H_{22}N_2O_2$
Formula weight	201.3	215.3	263.3	278.4	267.3	296.4	310.4
Wavelength/Å	1.5418	1.5418	1.5418	0.71069	1.5418	0.71069	1.5418
Source	CuK_α	CuK_α	CuK_α	MoK_α	CuK_α	MoK_α	CuK_α
T/K	293	293	293	293	293	293	293
a/Å	23.278(1)	23.9509(8)	25.0197(10)	13.593(2)	14.6191(7)	6.876(1)	20.528(1)
b/Å	23.278(1)	23.9509(8)	8.2920(5)	13.565(2)	7.1804(5)	7.661(1)	9.919(1)
c/Å	7.5723(6)	7.5527(5)	7.0353(3)	16.869(2)	26.633(2)	29.823(4)	16.885(2)
α/°							
β/°			94.849(5)	95.65(1)	98.203(6)	93.28(1)	102.331(8)
γ/°							
V/Å^3	3553.4(4)	3752.1(4)	1454.3(1)	3095.3(7)	2767.1(3)	1568.4(4)	3358.8(6)
Crystal size/mm^3	0.18 × 0.18 × 0.38	0.13 × 0.23 × 0.50	0.23 × 0.28 × 0.35	0.20 × 0.23 × 0.30	0.13 × 0.30 × 0.60	0.23 × 0.38 × 0.38	0.10 × 0.33 × 0.38
Crystal system	Hexagonal	Hexagonal	Monoclinic	Monoclinic	Monoclinic	Monoclinic	Monoclinic
Space group	*P*6*cc*	*P*6*cc*	$P2_1/n$	$P2_1/c$	*C*2/*c*	$P2_1/c$	$P2_1/n$
Z	12	12	4	8	8	4	8
D_x/g cm^{-3}	1.13	1.14	1.20	1.19	1.28	1.26	1.23
μ/mm^{-1}	0.56	0.56	0.57	0.07	0.73	0.08	0.64
F(000)	1296	1392	560	1184	1120	632	1328
θ Range/°	3.8 – 69.8	3.7 – 24.8	3.5 – 69.8	1.5 – 24.9	3.3 – 69.8	1.4 – 29.9	3.1 – 54.9
Measured refs.	1221	1164	2749	5393	2607	4522	4112
Obs. refs. ($I > 2.5\sigma(I)$)	987	865	2199	2582	2126	1972	2844
Refined parameters	137	146	182	380	182	199	416
G	26511(1532)	18135(1117)	3523(101)	12632(383)	2786(94)	-	350(70)
R[a])	0.054	0.052	0.041	0.052	0.055	0.065	0.125[d])
R_w[b])	0.071	0.065	0.037	0.050	0.054	0.061	0.122
A, B, C[c])	2.0, 0.01, 0.01	2.5, 0.01, 0.01	1.0,0.01,0.01	2.0, 0.01, 0.01	2.0,0.01,0.01	1.5,0.01,0.01	15.0,0.01,0.01
Goodness-of-fit	1.06	0.98	1.04	0.94	1.08	0.94	0.92
$\Delta\rho$ (max,min)/eÅ^{-3}	0.18, −0.25	0.22, −0.26	0.21, −0.15	0.35, −0.39	0.38, −0.31	0.53, −0.48	2.01, −0.84[d])
CCDC Deposition No.	191548	191549	191550	191551	191552	191553	191554

[a]) $R = \Sigma(|F_{obs}| - k|F_{calc}|)/\Sigma(|F_{obs}|)$. [b]) $R_w = \Sigma w(|F_{obs}| - k|F_{calc}|)^2/\Sigma(|F_{obs}|^2)$. [c]) $w^{-1} = (A + B\ (\sigma(F_{obs}))^2 + C/(\sigma(F_{obs})))$. [d]) Substantial residual electron density was found around the CN and MeOCO groups between the independent molecules **3T3A** and **3T3B**. All attempts to fit this to a disordered model were unsuccessful.

Table 2. *Selected Bond Lengths* [Å] *and Angles* [°] *with Estimated Standard Deviations in Parentheses.* Σ is the sum of the bond angles at N(1). Data for **1T2** and **4T2** are taken from [4]. For **1T2**, values in italics indicate that it is equal to that on the line above by symmetry.

	1T1	**2T1**	**1T2A**	**1T2B**	**2T2**	**3T2A**	**3T2B**	**4T2**	**5T2**	**2T3**	**3T3A**	**3T3B**
N(1)–C(2)	1.47(3)	1.477(10)	1.458(2)	1.467(2)	1.462(2)	1.470(5)	1.469(5)	1.464(2)	1.469(3)	1.474(5)	1.487(13)	1.471(13)
N(1)–C(6)	1.496(8)	1.49(4)	*1.458(2)*	*1.467(2)*	1.463(2)	1.465(5)	1.468(5)	1.460(2)	1.470(3)	1.470(5)	1.464(15)	1.467(14)
N(1)–C(10)	1.391(16)	1.399(16)	1.406(2)	1.401(2)	1.409(2)	1.414(5)	1.405(5)	1.413(1)	1.397(3)	1.411(5)	1.395(13)	1.390(12)
C(2)–C(3)	1.53(3)	1.56(3)	1.559(2)	1.538(2)	1.550(3)	1.554(6)	1.549(7)	1.550(2)	1.553(4)	1.556(6)	1.530(15)	1.555(14)
C(5)–C(6)	1.52(3)	1.54(3)	*1.559(2)*	*1.538(2)*	1.552(3)	1.540(6)	1.553(7)	1.546(2)	1.549(4)	1.548(5)	1.565(16)	1.536(14)
C(3)–C(4)	1.521(10)	1.50(4)	1.493(2)	1.505(2)	1.496(3)	1.498(6)	1.499(6)	1.502(2)	1.507(4)	1.505(6)	1.505(17)	1.473(16)
C(4)–C(5)	1.49(4)	1.516(12)	*1.493(2)*	*1.505(2)*	1.497(2)	1.507(6)	1.501(6)	1.496(2)	1.504(4)	1.508(6)	1.501(14)	1.521(14)
C(2)–N(1)–C(6)	102.7(15)	103.2(15)	104.1(1)	103.4(1)	103.7(1)	103.9(3)	103.4(3)	103.4(1)	103.3(2)	103.1(3)	103.9(8)	102.8(7)
C(2)–N(1)–C(10)	121.2(14)	121.9(11)	121.9(1)	121.5(1)	121.5(1)	120.6(3)	121.9(3)	120.7(1)	120.9(2)	120.9(3)	120.5(9)	121.9(8)
C(6)–N(1)–C(10)	120.7(11)	120.1(15)	*121.9(1)*	*121.5(1)*	120.0(2)	120.5(3)	121.7(3)	122.0(1)	121.4(2)	120.0(3)	120.7(9)	121.7(9)
Σ	345(2)	345(2)	347.9(2)	346.4(2)	345.2(2)	345.0(5)	347.0(5)	346.1(2)	345.6(3)	344.0(5)	345.1(15)	346.4(14)

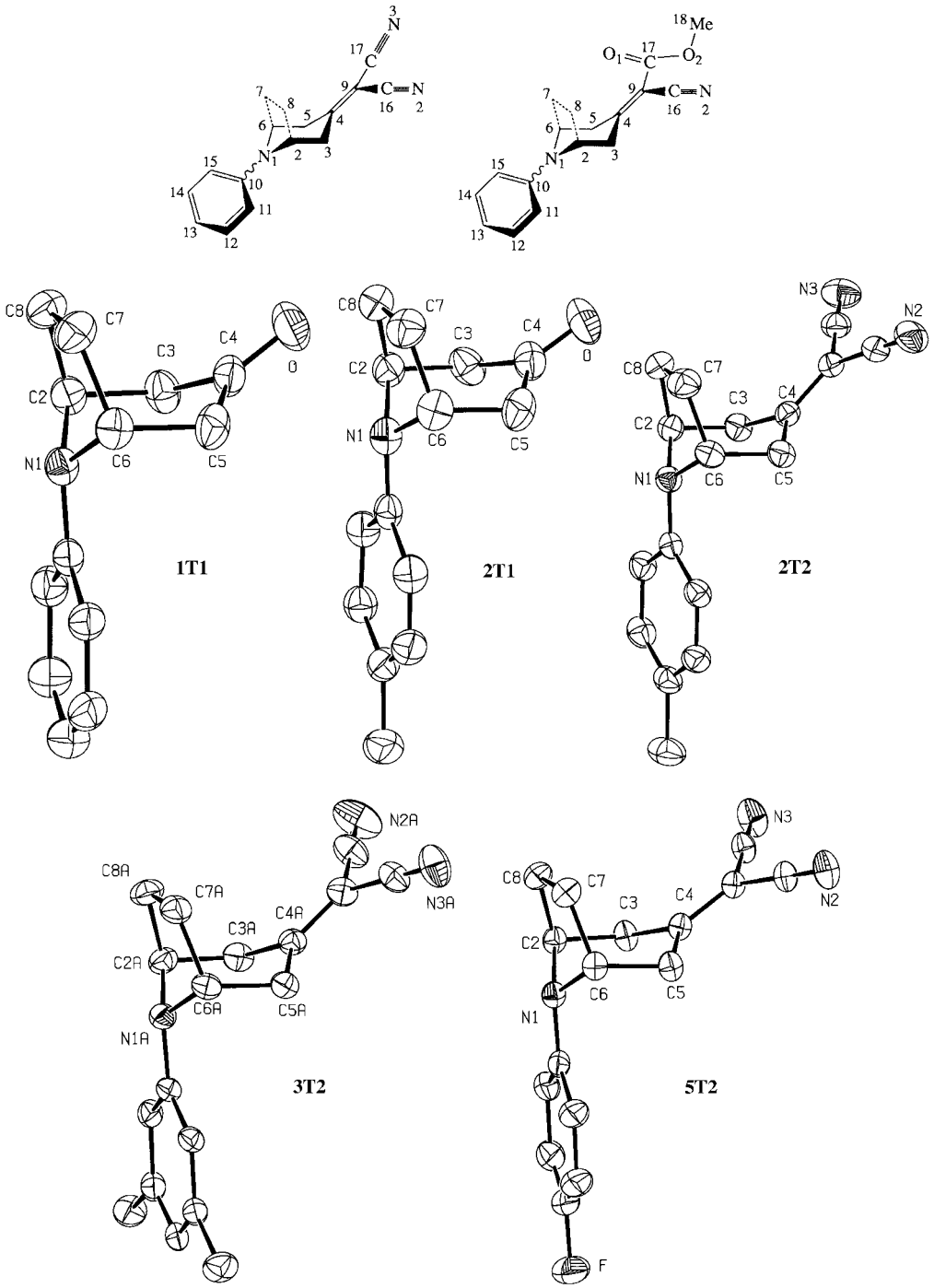

Fig. 2. *Atom-numbering* (arbitrary) *scheme in* **nTm**, *and ORTEP* [23] *drawings of* **1T1**, **2T1**, **2T2**, **3T2**, **5T2**, **2T3**, *and* **3T3**. The shapes of the ellipsoids correspond to 30% probability contours of atomic displacement. The H-atoms have been omitted for clarity.

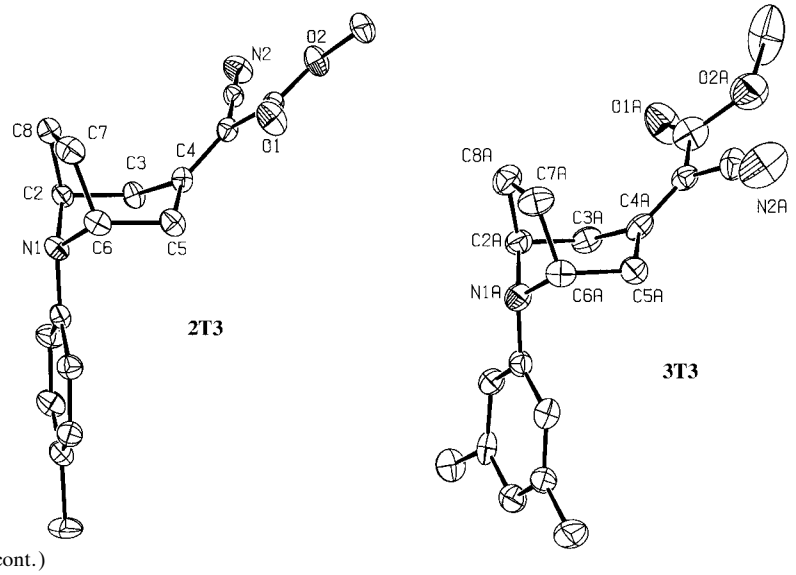

Fig. 2 (cont.)

first, and the parameters introduced for the **nPm** derivatives [3] were calculated (*Table 3*).

Analogous to the **nPm** derivates [3], the piperidine ring in the **nTm** X-ray structures is found in a chair conformation (*Fig. 2*).

Compound **1T2B**, and to a lesser extent **5T2**, and the ketones **1T1** and **2T1**, show a flattening of the C(2) – C(6) part of the molecule, leading to a decrease of both the angle between the planes *a* and *b*, and the distance of C(4) to plane *a*. A possible explanation for the flattening in **1T2B**, and its influence on the TBI between donor and acceptor, is given by *Krijnen et al.* [4].

In tropane-like systems, such a flattening of the C(2) – C(6) part of the molecule has also been reported for a few X-ray structures [11] and in solution [7][9][12]. The data collected in *Table 3*, however, indicate that, in our compounds, a nonflattened orientation of the C(2) – C(6) part of the molecules is preferred.

Table 3. *Angles* [°] *between Calculated Least-Squares Planes and Distances* [Å] *of N(1) and C(4) to the Central Plane* a *Defined by C(2), C(3), C(5), and C(6); Plane* b *Defined by C(3), C(4), and C(5)*; *Plane* c *Defined by C(2), N(1),* and *C(6)*. Data for **1T2** and **4T2** are taken from [4]; e.s.d.'s calculated with XTAL3.7 [21] from CIF. Asymmetry parameter ΔC_s calculated according to *Duax et al.* [13].

	1T1	**2T1**	**1T2A**	**1T2B**	**2T2**	**3T2A**	**3T2B**	**4T2**	**5T2**	**2T3**	**3T3A**	**3T3B**
Angle between planes *a* and *b*	37(3)	36(3)	46.3(2)	23.7(2)	43.9(2)	41.6(4)	46.3(4)	42.1(2)	36.1(3)	45.8(4)	43.0(10)	42.3(9)
Angle between planes *a* and *c*	62(2)	63(2)	62.9(2)	64.7(2)	62.8(2)	63.3(3)	63.8(3)	63.1(1)	64.1(3)	61.8(3)	62.4(8)	61.4(8)
Distance N(1) to plane *a*	−0.82(3)	−0.82(3)	−0.798(4)	−0.823(4)	−0.803(2)	−0.807(5)	−0.816(5)	−0.808(2)	−0.820(3)	−0.808(5)	−0.800(12)	−0.809(11)
Distance C(4) to plane *a*	0.49(4)	0.47(4)	0.580(3)	0.310(3)	0.557(3)	0.536(6)	0.587(6)	0.538(2)	0.467(4)	0.592(6)	0.565(15)	0.552(13)
ΔC_s	1.4	0.8	0	0	2.1	0.3	1.1	1.9	1.7	2.3	3.2	1.6

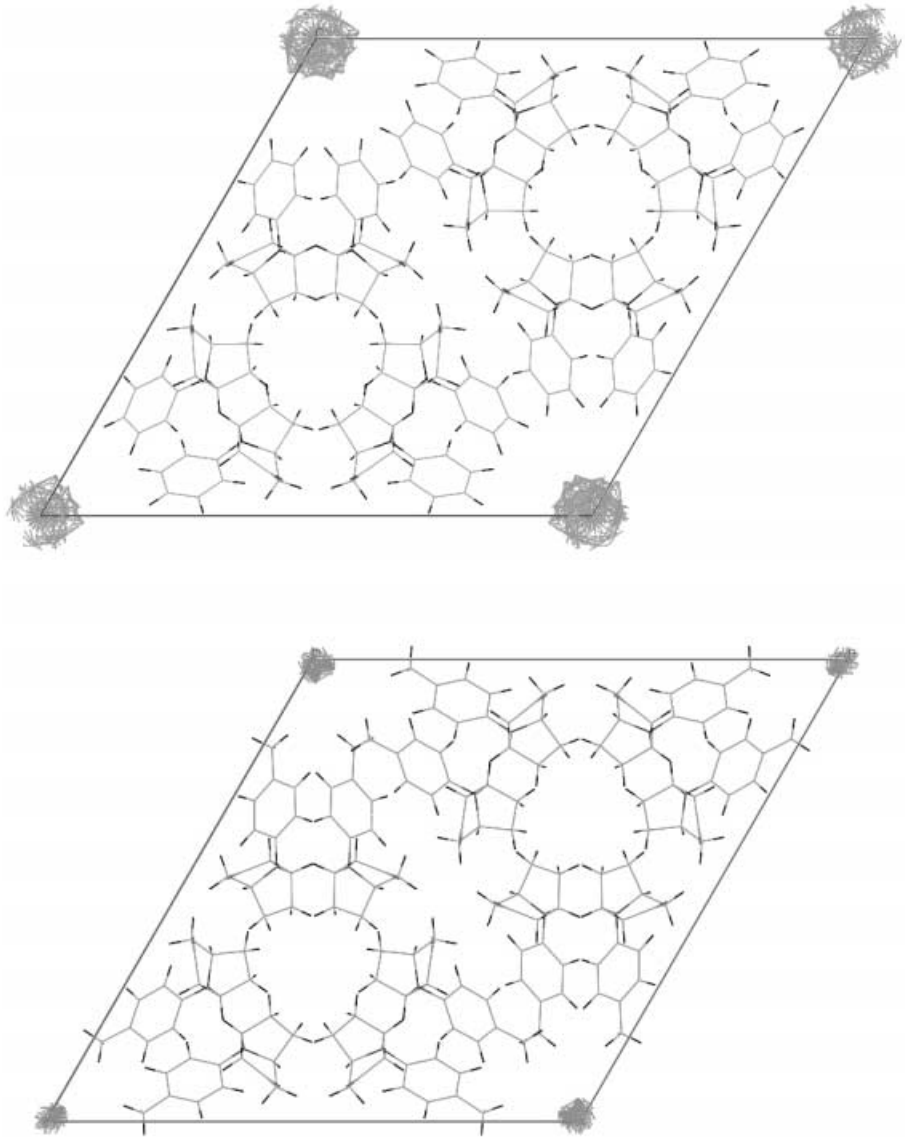

Fig. 3. *Unit cell of* **1T1** (top) *and* **2T1** (bottom), *viewed along the* c*-axis, showing the crystal packing.* The column-like residual electron density after refinement (before application of the SQUEEZE procedure of PLATON [23]) along the *c*-axis is indicated. PLATON [23] calculates a solvent accessible void near the origin of 351 Å^3 for **1T1** and 206 Å^3 for **2T1**.

Like in the **nPm** series [3], the orientation of the C(2)–N(1)–C(6) part of the molecule is fairly constant throughout the **nTm** series, the range of the angle between planes *a* and *c* being small. However, the introduction of the $-CH_2CH_2-$ bridge across

C(2) and C(6) in the **nTm** compounds slightly increases the angle between the planes *a* and *c*, and the distance of N(1) to plane *a:* for the **nTm** compounds, the averages are 62.9(9)° and −0.81(1) Å *vs.* 53.7(10)° and −0.67(2) Å for the **nPm** compounds.

Analogous to the **nPm** structures [3], it has to be expected that, in the **nT2** structures, the piperidine ring displays (near) C_s symmetry. Deviations from this (quasi) C_s symmetry can occur when the aryl group is strongly twisted around the N(1)–aryl bond by an asymmetry in the acceptor part of the molecule, *e.g.*, an asymmetrically substituted exocyclic C=C bond in the **nT3** structures, or by distortions of the solid-state structure due to crystal-packing effects. The asymmetry parameters (*Table 3*) defined by *Duax et al.* [13] indicate that the deviations from (quasi) C_s symmetry are very small, indicating that the piperidine ring adopts a normal chair conformation. The calculated ΔC_s values are comparable to those calculated for the **nPm** compounds [3].

Inspection of the C(2)–C(3) and C(5)–C(6) bond lengths (*Table 2*) reveals deviation from C_s symmetry in **3T2A**. This asymmetry is probably caused by crystal-packing effects, because neither a pronounced twist of the aryl group around the N(1)–aryl bond (see *Sect. 2.4*), nor a significant amount of asymmetry in the acceptor part of the molecule (see *Sect. 2.5*) have been found. In the other **nT2** structures, the piperidine-ring bond lengths (*Table 2*) indicate that the piperidine ring is highly symmetric. In contrast, the structure containing the asymmetric acceptor chromophore, **3T3**, is indeed asymmetric, especially through the central C(2)–C(3) and C(6)–C(5) bonds (*Table 2*).

2.4. *Configuration at the Piperidine N-Atom*. The sum of the bond angles at N(1) (*Table 2*) is fairly constant (344.0(5)–347.9(2)°), indicating that the piperidine N-atom N(1) adopts a flattened pyramidal configuration in all compounds. In the **nTm** series, the C(2)–N(1)–C(6) angle (102.7(15)–104.1(1)°) is significantly smaller than in the **nPm** compounds (109.6(3)–112.6(2)°) [3] as the result of the $-CH_2CH_2-$ bridge across C(2) and C(6) in the tropanone derivatives.

From selected torsion angles along the N(1)–C(10) bond, the twist angle β, which is a measure of the deviation from complete alignment of the N-atom lone pair and the aromatic π-system, can be calculated (*Table 4*). β indicates how the aryl group is orientated with respect to the piperidine ring: when $\beta = 0$, then the plane through the aryl C-atoms is perpendicular to the mirror plane of the piperidine ring.

In the **nTm** structures, only a small spread in β (0–9.0(1)°) is found (*Table 4*), and this range is significantly smaller than the $\beta \approx 24°$ predicted from AM1 calculations for **1P2** [2]. This indicates that, in the axial conformation, a preference exists for maximum overlap of the N-atom lone pair and the aromatic π-system. In such a conformation, the plane through the aromatic C-atoms is perpendicular to the mirror plane of the piperidine ring, which is very similar to the preferred orientation reported for the Ph group in the axial conformation of, *e.g.*, phenylcyclohexane and related compounds [14].

Table 4. *Absolute Values of Selected Torsion Angles* [°] *along the N(1)–C(10) Bond and Calculated Values of the Twist Angles* β. Data for **1T2** and **4T2** are taken from [4]; e.s.d.'s calculated with XTAL3.7 [21] from CIF. For **1T2**, $\tau_1 = \tau_2$ by symmetry.

	1T1	**2T1**	**1T2A**	**1T2B**	**2T2**	**3T2A**	**3T2B**	**4T2**	**5T2**	**2T3**	**3T3A**	**3T3B**
C(2)–N(1)–C(10)–C(11) (τ_1)	23(3)	27(4)	23.9(4)	25.0(4)	18.1(2)	23.2(6)	25.0(6)	34.6(2)	32.4(4)	35.1(5)	31.4(13)	27.2(13)
C(6)–N(1)–C(10)–C(15) (τ_2)	31(3)	26(3)	*23.9(4)*	*25.0(4)*	33.1(2)	27.1(5)	25.6(6)	16.7(2)	17.8(4)	18.3(5)	20.7(13)	21.9(12)
$\beta = 1/2 \vert\vert \tau_1 \vert - \vert \tau_2 \vert \vert\vert$	4(2)	1(3)	0	0	7.5(1)	2.0(4)	0.3(4)	9.0(1)	7.3(3)	8.4(4)	5.4(9)	2.7(9)

In contrast to the **nPm** structures [3], there is no correlation between the sum of the bond angles Σ at N(1) and the twist angle β and between Σ and bond length N(1)–C(10), respectively (correlation coefficient -0.54, and -0.05, resp.). This is to be expected since the Ph ring is invariably in the axial orientation.

2.5. *Elongation of the 'Central' C–C bond under the Influence of TBI*. In the solid state, TBI between two functionalities may result in elongation of the central C–C bond in the σ-frame connecting these functionalities [15]. In the **nTm** compounds, TBI could, thus, manifest itself *via* elongation of the C(2)–C(3) and C(5)–C(6) bonds.

In the aforementioned X-ray structures of tropane-like compounds (see *Sect. 2.1*) found *via* computer search in the *CSD* [5], the average length of the central C–C bond in the piperidine ring is 1.528(2) Å, irrespective of the equatorial or axial orientation of the *N*-substituent. This is slightly longer than the mean value of 1.509(1) Å found for 314 piperidine derivatives in the *CSD*. The difference is probably due to the introduction of the $-CH_2CH_2-$ bridge across C(2) and C(6) in the tropane derivatives. The observed central bond length of 1.559(2) Å in **1T2A** (*Table 2*) is, therefore, significantly longer than normal, and was claimed by *Krijnen et al.* [4] to be one of the first examples of bond elongation related to TBI over three σ-bonds in relatively simple unstrained organic molecules! The presence of two different structures of **1T2** in one and the same crystal (and, therefore, obtained under completely identical conditions!) affords a unique opportunity to establish the effect of TBI on bond lengths. As mentioned in *Sect. 2.3*, the flattening of the C(2)–C(6) part of the molecule in **1T2B** should result in a decrease in TBI between the donor and acceptor. The length of the central C–C bond in **1T2B** (1.538(2) Å) is not only significantly smaller than in **1T2A**, but is comparable to the normal value for tropane derivatives. This observation offers another very convincing example of the very subtle conformational requirements of TBI.

Based on AM1 calculations, *Krijnen* [2] concluded that TBI between the donor and acceptor decreases in the order **1Tm** > **3Tm** > **2Tm** ≈ **5Tm** > **4Tm**. If the length of the central C–C bond is indeed controlled by TBI between the donor and acceptor, modifications of this interaction should result in a modification of the central bond length. The structures **1T2A**, **2T2**, **3T2B**, **4T2**, and **5T2** can be compared nicely because both the configuration and the symmetry of the central piperidine ring are essentially the same in these structures (*cf. Sect. 2.3*). Inspection of the central C–C bond length of **4T2** (mean value 1.548(1) Å) reveals that this bond is shorter than in **1T2A** (1.559(2) Å), thus indicating that the length of the central C–C bond is indeed controlled by TBI! The mean value of the C–C bond length of **3T2B**, **2T2**, and **5T2** are between those of **1T2A** and **4T2**. The central C–C bond length in **3T2A** (mean value 1.549(3) Å) is probably influenced by distortions in the solid state (*cf. Sect. 2.3*), and, consequently, not directly comparable to the bond lengths found in **1T2A**, **2T2**, **3T2B**, **4T2**, and **5T2**. Finally, the central C–C bond length in **1T2B** (1.538(2) Å) is the shortest, but the C(2)–C(6) part in **1T2B** is significantly flattened (*cf. Table 3*), and such flattening results in a decrease of the influence of TBI on the length of the central bond.

2.6. *Pyramidalization at C(4)*. To study the pyramidalization at C(4) of the piperidine ring, the torsion angles along the C(4)–C(9), C(3)–C(4), and C(5)–C(4) bonds were calculated (*Table 5*). The flattening of the C(2)–C(6) part of the molecule noted previously for **1T2B** and **5T2** (*cf. Sect. 2.1*) is nicely reflected in an increase of the

torsion angles $H_{eq}-C(3)-C(4)-C(9)$ and $H_{eq}-C(5)-C(4)-C(9)$ and a decrease of the torsion angles $C(2)-C(3)-C(4)-C(5)$ and $C(6)-C(5)-C(4)-C(3)$ compared to the other structures.

Slight deviations from planarity have often been observed in substituted alkenes [16] when the two alkene C-atoms and the four attached atoms cannot define a plane of molecular symmetry. The torsion angles along the $C(4)-C(9)$ bond (*Table 5*) indicate significant non-coplanarity in the acceptor moiety: in the case of coplanarity, $C(3)-C(4)-C(9)-C(16)$ and $C(5)-C(4)-C(9)-C(17)$ should be equal to zero.

Two types of distortions from the ideal planar geometry can occur: twisting around the $C(4)-C(9)$ bond and pyramidalization at C(4). For example, **4T2** and **2T3** show slight twisting around the $C(4)-C(9)$ bond, which may be attributed to crystal-packing effects.

Fig. 4 shows that the pyramidalization at C(4) can, *a priori*, direct C(9) in two different directions. The angle θ (*Fig. 4*) is a measure for the degree and direction of the pyramidalization at C(4): $\theta < 0$ indicates equatorial bending of C(9) and $\theta > 0$ bending in the axial direction.

Theoretical studies on alkenes and carbonyls [16][17] predict that the C-atom will pyramidalize toward a staggered geometry to relieve torsional interactions between the allylic bonds and the two σ-bonds and π-orbitals attached to the alkene C-atom. Such a pyramidalization toward the bond most parallel to the π-system is confirmed by a survey of neutron-diffraction crystal structures of amino acids and dipeptides [17]. For the **nTm** compounds, this would correspond to bending C(9) in the equatorial direction, thus toward $H_{ax}-C(3)$ and $H_{ax}-C(5)$ ($\theta < 0$).

In *Table 5*, the values for θ, obtained by averaging the θ values determined from the torsion angles along the $C(3)-C(4)$ and $C(5)-C(4)$ bonds, are listed. The expected negative pyramidalization is found only in **1T2B** ($\theta = -5^\circ$). As mentioned in *Sect. 2.3*,

Table 5. *Absolute Values of Selected Torsion Angles* [°] *along the C(4)–C(9), C(3)–C(4), and C(5)–C(4) Bonds for the Compounds* **nT2** and **nT3**. Data for **1T2** and **4T2** are taken from [4]; e.s.d.'s calculated with XTAL3.7 [21] from CIF. For **1T2**, the torsion angles along the C(5)–C(4) bond (in italics) are equal to the equivalent ones along C(3)–C(4) by symmetry.

	1T2A	**1T2B**	**2T2**	**3T2A**	**3T2B**	**4T2**	**5T2**	**2T3**	**3T3A**	**3T3B**
Along C(4)–C(9)										
C(3)–C(4)–C(9)–C(16)	3.4(5)	1.0(4)	1.3(3)	3.5(7)	1.1(7)	0.2(2)	1.5(4)	4.4(6)	3.9(16)	1.8(16)
C(5)–C(4)–C(9)–C(17)	3.4(5)	1.0(4)	3.8(3)	2.3(7)	6.8(7)	4.7(3)	1.9(4)	6.5(5)	1.3(16)	1.6(15)
Along C(3)–C(4)										
C(2)–C(3)–C(4)–C(5)	49.4(2)	25.8(3)	46.3(2)	44.8(5)	49.3(5)	45.7(2)	39.4(3)	48.3(4)	48.7(11)	45.3(11)
$H_{eq}-C(3)-C(4)-C(9)$	3	39	7.4(2)	13.1(6)	4.2(6)	9	19.2(4)	8.4(6)	4.2(15)	11.7(14)
$H_{ax}-C(3)-C(4)-C(5)$ (τ_a)	70	95	74.2(2)	75.5(5)	70.5(5)	72	81.4(3)	71.7(4)	71.1(11)	75.7(10)
$H_{ax}-C(3)-C(4)-C(9)$ (τ_b)	118	80	111.3(2)	106.9(5)	116.5(5)	112	99.3(3)	110.4(4)	113.3(11)	106.0(11)
$\Sigma_1 = \lvert\tau_a\rvert + \lvert\tau_b\rvert$	188	175	185.5(3)	182.4(7)	187.0(7)	184	180.7(4)	182.1(6)	184.4(16)	181.7(15)
Along C(5)–C(4)										
C(6)–C(5)–C(4)–C(3)	*49.4(2)*	*25.8(3)*	47.5(2)	44.7(5)	49.6(5)	44.5(2)	38.3(3)	49.8(4)	45.3(12)	45.9(11)
$H_{eq}-C(5)-C(4)-C(9)$	*3*	*39*	6.9(2)	12.2(6)	3.6(6)	14	19.7(4)	7.9(5)	8.4(15)	11.2(14)
$H_{ax}-C(5)-C(4)-C(3)$ (τ_c)	*70*	*95*	73.9(2)	75.2(5)	70.1(5)	76	82.0(3)	70.9(4)	75.8(11)	75.1(11)
$H_{ax}-C(5)-C(4)-C(9)$ (τ_d)	*118*	*80*	111.5(2)	107.2(5)	116.9(5)	108	98.7(3)	111.0(4)	108.6(12)	106.6(11)
$\Sigma_2 = \lvert\tau_c\rvert + \lvert\tau_d\rvert$	188	175	185.4(3)	182.4(7)	187.0(7)	184	180.7(4)	181.9(6)	184.4(16)	181.7(16)
$\theta = 1/2\ (\Sigma_1 + \Sigma_2) - 180^\circ$	8	−5	5.5(2)	2.4(5)	7.0(5)	4	0.7(3)	2.0(4)	4.4(11)	1.7(11)

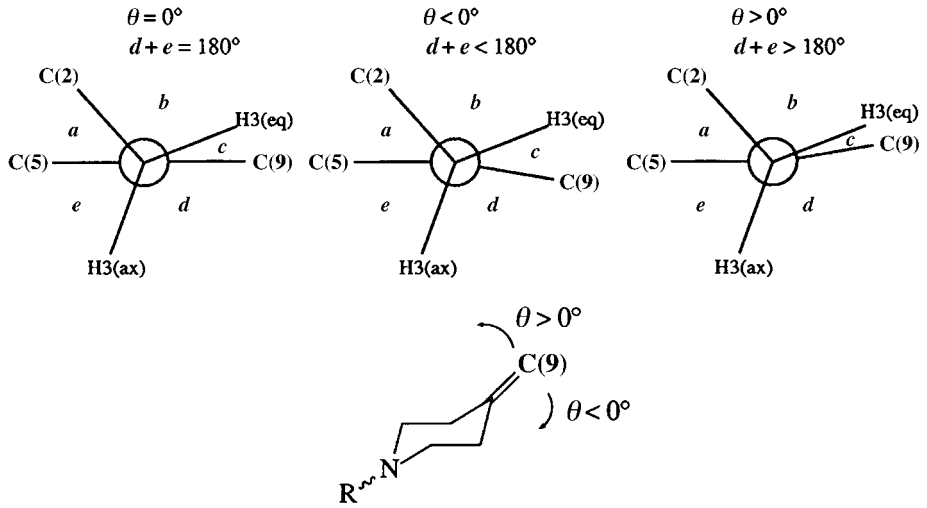

Fig. 4. *Possible modes of pyramidalization at C(4) and the corresponding* Newman *projections along the* C(3)–C(4) bond. $\theta = (d + e) - 180°$.

the C(2)–C(6) part of this structure is flattened, resulting in a decrease of TBI. In all the other **nTm** structures, pyramidalization with a positive θ is found, even up to $+8°$. This observation is in strong contrast to the above prediction based on relief of torsional interactions.

Pyramidalization at C(4) into the axial direction ($\theta > 0°$) leads to greater electron density in the π-orbital of C(4) into the equatorial direction. Consequently, the π-lobe on C(4) becomes more antiparallel to the central C–C bond, thus enabling more-effective coupling of the acceptor with the N(1) lone pair. Such donor–acceptor interactions result in an enthalpic stabilization of the molecular system. Therefore, the energetically unfavorable distortion of the C=C bond, *i.e.*, the bending of C(9) resulting in a pyramidalization at C(4) with $\theta > 0°$, is probably compensated by a stabilization offered by the increase in donor–acceptor interaction upon such a pyramidalization.

For the structures compared in *Sect. 2.5*, the pyramidalization at C(4) decreases in the order **1T2A** > **3T2B** > **2T2** > **4T2** > **5T2**. Probably, the unexpectedly low value of **5T2** can be explained by the fact that some flattening of the piperidine ring was observed (*cf. Sect. 2.3*). That **1T2A**, the structure with the strongest TBI judged from the elongation of the central C–C bond, displays also the strongest pyramidalization in the **nTm** series further supports the idea that, in these compounds, this pyramidalization is correlated with TBI and not merely with crystal-packing effects. This is also supported by the observation that the pyramidalization at C(4) is smaller in **2T3** compared to **2T2**, and smaller in **3T3B** compared to **3T2B**; again, this might be correlated to a decrease of TBI between the donor and acceptor chromophores as a consequence of the acceptor modification.

The observed pyramidalization of at most $+8°$ may seem small compared to the pyramidalization of the central C=C bond found in some derivatives of *syn*-

sesquinorbornene, which amounts to up to 22° [18], but it reflects interactions in the ground-state of the molecules, which are, according to *Houk* and co-workers [16], related to much larger energetic effects occurring in transition states for addition reactions. *Gleiter* [19] correlated the observed pyramidalization, *e.g.*, for derivatives of *syn*-sesquinorbornene and related compounds to the experimental stereoselectivity in addition reactions to these compounds. Although the observed pyramidalization at C(4) in the donor–acceptor compounds **nTm** is significantly smaller than that reported for derivatives of *syn*-sesquinorbornene, it still could be anticipated that this pyramidalization, and, thus, TBI, could have a pronounced influence on the stereoselectivity in addition reactions to the acceptor C=C bond, an effect worthwhile to be investigated in the near future.

3. Conclusions. – In all available X-ray structures of **nTm** compounds, the aryl group is found in an axial orientation. When the piperidine ring adopts a normal chair conformation, significant elongation of the central C–C bond is observed, thus confirming the effect of through-bond interaction on the length of the central C–C bond. Flattening of the C(2)–C(6) part of the molecule reduces elongation of the central bond, thus indicating that TBI depends very strongly on the conformation of the molecular system.

The donor–acceptor interaction influences not only the length of the central C–C bond but also the pyramidalization at C(4). The X-ray structures indicate that, in general, the degree and direction of this pyramidalization is mainly controlled by TBI. In structures with strong TBI – judged from a pronounced elongation of the central C–C bond – the pyramidalization at C(4) (up to 8° in **1T2A**) directs C(9) in the axial direction. In structures with less-pronounced TBI – due to a pronounced flattening of the C(2)–C(6) part of the molecule – this pyramidalization is reduced.

Experimental Part

1. *X-Ray Crystal-Structure Determination.* The reflections were collected on an *Enraf-Nonius CAD-4* diffractometer with graphite-monochromated CuK_α or MoK_α radiation (*Table 1*). The unit-cell dimensions resulted from a least-squares fit of the setting angles of 23 centered reflections. The structures were solved by CRUNCH [20] and refined with XTAL3.7 [21]. Full-matrix least-squares refinement was used, anisotropic for non-H-atoms and isotropic for H-atoms. The H-atoms were kept fixed at their calculated positions with fixed $U_{eq} = 0.10$ Å^2. An extinction correction [22] but no absorption correction was applied.

A final difference *Fourier* map revealed a maximum and minimum electron density of 0.60 and -0.21 eÅ^{-3} for **1T1**, and of 1.13 and -0.28 eÅ^{-3} for **2T1** (*Fig. 3*). Since the solvent molecules could not be modeled, the SQUEEZE procedure of PLATON [23] was applied. The compensated electron counts per cell were 45 and 37 for **1T1** and **2T1**, resp. For both structures, two solvents were used in the recrystallization procedure. The number of electrons of these solvents does not correspond to the above-mentioned compensated electron count per cell. Therefore, no account could be made with respect to the empirical formula, formula weight, density, μ, and $F(000)$ of these two crystal structures.

The crystallographic data (excluding structure factors) of all new structures presented in *Table 1* and *Fig. 2* [23] have been deposited with the *Cambridge Crystallographic Data Centre* (*CCDC*); deposition Nos. are given in *Table 1*. Copies of the data can be obtained, free of charge, on application to the *CCDC*, 12 Union Road, Cambridge, CB21EZ, UK (fax: +44-1223-336033; e-mail: deposit@ccdc.cam.ac.uk).

2. *Syntheses.* The compounds can be synthesized by *Knoevenagel*-type condensation [24] of malononitrile (to give the **nT2** compounds) or methyl cyanoacetate (to give the **nT3** compounds), and the appropriate ketones **nT1** (*Scheme*).

2.1. *Synthesis of* N-*Aryltropanones* **nT1**. The synthesis of **1T1** and **4T1** was already reported by *Krijnen et al.* [4]. Since this approach was time-consuming (because the purification of the cyclohepta-2,6-dienone was

troublesome), an alternative route has been developed based on the *Robinson-Schöpf* synthesis of *N*-methyltropanone [25].

2.1.1. *8-Phenyl-8-azabicyclo[3.2.1]octan-3-one* (**1T1**). After refluxing a mixture of 2,3,4,5-tetrahydro-2,5-dimethoxyfuran (4.81 g, 36.4 mmol) and 0.1 ml of conc. H_2SO_4 in 30 ml of H_2O for 30 min, this mixture was added to a soln. prepared from 3-oxopentanedioic acid (11.00 g, 75.5 mmol), AcONa (18.00 g), and freshly distilled aniline (3.38 g, 36.3 mmol) in 500 ml of H_2O. The mixture was allowed to stand at r.t. overnight. The solid that separated was collected by filtration and dissolved in 250 ml of a 5% HCl soln. at 60°. After cooling in an ice bath, it was made basic (pH 9–10) with NH_3. The solid that separated was collected and recrystallized from MeOH/H_2O 4:1 to yield **1T1**. Off-white solid. Total yield: 3.13 g (15.6 mmol, 43% with respect to 2,3,4,5-tetrahydro-2,5-dimethoxyfuran). M.p. 101–103° ([9]: 107–108°, [26]: 107–109°, [27]: 103°) (crystals suitable for X-ray analysis were obtained by slow evaporation of a CH_2Cl_2/hexane soln. (M.p. 101–102.5°)). IR ($CHCl_3$): 3030*w*, 3000*w*, 2960*w*, 1705*s*, 1590*s*, 1495*s*, 685*m*. ^{1}H NMR (250 MHz, $CDCl_3$): 7.30 (*m*, H–C(3), H–C(5) of Ph); 6.83 (*m*, H–C(2), H–C(4), H–C(6) of Ph); 4.48 (*m*, H–C(1), H–C(5)); 2.68 (*dd*, $J \approx 15.0$, 4.6, H_{ax}–C(2), H_{ax}–C(4)); 2.30 (*dd*, $J \approx 15.0$, 1.0, H_{eq}–C(2), H_{eq}–C(4)); 2.18 (*m*, H_{exo}–C(6), H_{exo}–C(7)); 1.78 (*dd*, $J \approx 14.4$, 7.0, H_{endo}–C(6), H_{endo}–C(7)). HR-MS: 201.1156 ($C_{13}H_{15}NO^+$; calc., 201.1154).

2.1.2. *8-(4-Methylphenyl)-8-azabicyclo[3.2.1]octan-3-one* (**2T1**). The succinaldehyde was prepared by refluxing 2,3,4,5-tetrahydro-2,5-dimethoxyfuran (7.26 g, 54.9 mmol) and 0.15 ml of conc. H_2SO_4 in 60 ml of H_2O for 30 min. This soln. was added to a mixture of 3-oxopentanedioic acid (24.25 g, 166.0 mmol), AcONa (22.01 g), and *p*-toluidine (7.85 g, 73.3 mmol) in 875 ml of H_2O. The same reaction time and workup as described for **1T1** yielded an almost white solid, which was recrystallized from MeOH/H_2O: 5.74 g (26.7 mmol, 49%) of **2T1**. M.p. 94–95° ([27]: 96°) (crystals suitable for X-ray analysis were obtained by slow evaporation of an Et_2O/CH_2Cl_2 soln. (m.p. 95–96°)). IR ($CHCl_3$): 3025*w*, 2990*m*, 2950*m*, 2915*m*, 2875*m*, 1700*s*, 1615*m*, 1505*s*, 805*m*. ^{1}H-NMR (200 MHz, $CDCl_3$): 7.12 (*d*, $J \approx 8.3$, H–C(3), H–C(5) of C_6H_4); 6.81 (*d*, $J \approx 8.5$, H–C(2), H–C(6) of C_6H_4); 4.47 (*m*, H–C(1), H–C(5)); 2.71 (*d* with additional fine coupling, H_{ax}–C(2), H_{ax}–C(6)); 2.29 (*d* with additional fine coupling, $J \approx 15.0$, H_{eq}–C(2), H_{eq}–C(6)); 2.29 (*s*, Me); 2.18 (*m*, H_{exo}–C(6), H_{exo}–C(7)); 1.78 (*dd*, $J \approx 14.4$, 7.0, H_{endo}–C(6), H_{endo}–C(7)).

2.1.3. *8-(3,5-Dimethylphenyl)-8-azabicyclo[3.2.1]octan-3-one* (**3T1**). The succinaldehyde was prepared by refluxing (30 min) 2,3,4,5-tetrahydro-2,5-dimethoxyfuran (6.15 g, 46.5 mmol) and 0.12 ml of conc. H_2SO_4 in 50 ml of H_2O. This soln. was added to a mixture of 3-oxopentanedioic acid (20.00 g, 136.9 mmol), AcONa (18.15 g), and 3,5-dimethylaniline (7.24 g, 59.7 mmol) in 720 ml of H_2O. The same reaction time and workup as for **1T1** yielded a white/cream-colored solid, which was recrystallized from MeOH/H_2O. This recrystallization yielded only 0.76 g of the desired off-white product **3T1**. Evaporation of the filtrate and subsequent recrystallization from hexane/Et_2O yielded much more of **3T1**. Total yield: 4.12 g (18.0 mmol, 39%). M.p. 140–142° (from hexane/Et_2O), 138–144° (from H_2O/MeOH). IR ($CHCl_3$): 3000*w*, 2960*m*, 2880*m*, 2850*w*, 1705*s*, 1595*s*, 825*m*. ^{1}H-NMR (200 MHz, $CDCl_3$): 6.52 (*s*, H–C(2), H–C(6) of C_6H_3); 6.50 (*s*, H–C(4) of C_6H_3); 4.49 (br. *s*, H–C(1), H–C(5)); 2.71 (*dd*, $J \approx 15.3$, 4.1, H_{ax}–C(2), H_{ax}–C(4)); 2.30 (*d*, $J \approx 15.1$, H_{eq}–C(2), H_{eq}–C(4)); 2.30 (*s*, Me); 2.16 (*m*, H_{exo}–C(6), H_{exo}–C(7)); 1.77 (*dd*, $J \approx 14.3$, 6.9, H_{endo}–C(6), H_{endo}–C(7)).

2.2. *Synthesis of the Donor–Acceptor Systems* **nT2** *and* **nT3**. 2.2.1. *2-[8-(4-Methylphenyl)-8-azabicyclo[3.2.1]octan-3-ylidene]propanedinitrile* (**2T2**) was prepared by refluxing **2T1** (0.50 g, 2.32 mmol), malononitrile (0.17 g, 2.57 mmol), 180 mg of $AcONH_4$, and 0.30 ml of AcOH in 5 ml of toluene for 2 h in a *Dean-Stark* apparatus. The usual workup (see [4]) yielded a yellow solid, which was purified by flash column chromatography (FC; silica gel; CH_2Cl_2). The product was finally recrystallized from Et_2O/CH_2Cl_2 to yield **2T2** as yellow crystals. Yield: 180 mg (0.68 mmol, 29%). M.p.: 180.5–181.5°. IR ($CHCl_3$): 3030*w*, 2955*m*, 2920*m*, 2880*w*, 2850*w*, 2230*m*, 1610*m*, 1585*m*, 1510*m*, 805*m*. ^{1}H-NMR (200 MHz, $CDCl_3$): 7.13 (*d*, $J \approx 8.4$, H–C(3), H–C(5) of C_6H_4); 6.77 (*d*, $J \approx 8.5$, H–C(2), H–C(6) of C_6H_4); 4.48 (br. *s*, H–C(1), H–C(5)); 2.86 (*d*, $J \approx 14.2$, H_{eq}–C(2), H_{eq}–C(4)); 2.75 (*dd*, $J \approx 15.0$, 3.3, H_{ax}–C(2), H_{ax}–C(4)); 2.28 (*s*, Me); 2.15 (*m*, H_{exo}–C(6), H_{exo}–C(7)); 1.68 (*dd*, $J \approx 14.5$, 6.8, H_{endo}–C(6), H_{endo}–C(7)). ^{13}C-NMR (50.3 MHz, APT, $CDCl_3$): 180.0 (C(3)); 141.9 (C(1) of C_6H_4); 130.5 (C(3), C(5) of C_6H_4); 128.6 (C(4) of C_6H_4); 115.1 (C(2), C(6) of C_6H_4); 111.6 (*C*N); 85.6 (C(3)=*C*); 55.7 (C(1), C(5)); 36.8 (C(2), C(4)); 28.5 (C(6), C(7)); 20.3 (Me). HR-MS: 263.1419 ($C_{17}H_{17}N_3^+$; calc. 263.1423).

2.2.2. *2-[8-(3,5-Dimethylphenyl)-8-azabicyclo[3.2.1]octan-3-ylidene]propanedinitrile* (**3T2**) was prepared by refluxing **3T1** (0.50 g, 2.18 mmol), malononitrile (0.16 g, 2.42 mmol), 167 mg of $AcONH_4$, and 0.39 ml of AcOH in 5 ml of toluene for 2 h in a *Dean-Stark* apparatus. The usual workup yielded a yellow solid, which was purified by filtration over a glass filter filled with silica and CH_2Cl_2 as eluent. After evaporation of the solvent, the isolated yellow solid was recrystallized by slow evaporation of an Et_2O/hexane soln. Yield of **3T2**: 379 mg (1.37 mmol, 63%). M.p. 218–219°. IR ($CHCl_3$): 3030*w*, 3000*m*, 2970*m*, 2920*m*, 2880*m*, 2230*m*, 1595*s*, 1585*s*,

825*m*, 685*m*. ^{1}H-NMR (200 MHz, $CDCl_3$): 6.53 (*s*, H–C(4) of C_6H_3); 6.49 (*s*, H–C(2), H–C(6) of C_6H_3); 4.49 (br. *s*, H–C(1), H–C(5)); 2.88 (*d* with additional fine coupling, $J \approx 15.1$, H_{eq}–C(2), H_{eq}–C(4)); 2.76 (*dd*, $J \approx$ 14.9, 3.1, H_{ax}–C(2), H_{ax}–C(4)); 2.30 (*s*, 2 Me); 2.15 (*m*, H_{exo}–C(6), H_{exo}–C(7)); 1.68 (*dd*, $J \approx 14.5$, 6.7, H_{endo}–C(6), H_{endo}–C(7)). ^{13}C-NMR (62.9 MHz, APT, $CDCl_3$): 180.0 (C(3)); 144.3 (C(1) of C_6H_3); 139.7 (C(3), C(5) of C_6H_3); 121.3 (C(4) of C_6H_3); 112.9 (C(2), C(6) of C_6H_3); 11.6 (CN), 85.7 (C(3)=*C*); 55.5 (C(1), C(5)); 37.2 (C(2), C(4)); 28.5 (C(6), C(7)); 21.7 (Me). HR-MS: 277.1584 ($C_{18}H_{19}N_3^+$; calc. 277.1579).

2.2.3. *2-[8-(4-Fluorphenyl)-8-azabicyclo[3.2.1]octan-3-ylidene]propanedinitrile* (**5T2**) was prepared by refluxing **5T1** (0.49 g, 2.23 mmol), malononitrile (0.16 g, 2.42 mmol), 167 mg of $AcONH_4$, and 0.39 ml of AcOH in 10 ml of toluene for 2 h in a *Dean-Stark* apparatus. After the usual workup, the product was purified by filtration over a glass filter filled with silica and CH_2Cl_2 as eluent and finally recrystallized from hexane/CH_2Cl_2 to yield **5T2** as yellow crystals. Yield: 147 mg (0.55 mmol, 25%). M.p. 145–146°. IR ($CHCl_3$): 3020*w*, 2970*m*, 2915*w*, 2875*w*, 2225*m*, 1580*m*, 1505*s*, 815*s*. ^{1}H-NMR (200 MHz, $CDCl_3$): 7.05 (*m*, H–C(3), H–C(5) of C_6H_4); 6.80 (*m*, H–C(2), H–C(6) of C_6H_4); 4.45 (br. *s*, H–C(3), H–C(5)); 2.88 (*d* with additional fine coupling, $J \approx$ 14.7, H_{eq}–C(2), H_{eq}–C(4)); 2.73 (*dd*, $J \approx 15.1$, 3.3, H_{ax}–C(2), H_{ax}–C(4)); 2.16 (*m*, H_{exo}–C(6), H_{exo}–C(7)); 1.70 (*dd*, $J \approx 14.6$, 6.8, H_{endo}–C(6), H_{endo}–C(7)). ^{13}C-NMR (50.3 MHz, APT, $CDCl_3$): 179.3 (C(3)); 156.8 (*d*, *J*(C,F) ≈ 238.9, C(4) of C_6H_4); 140.7 (C(1) of C_6H_4); 116.6 (*d*, *J*(C,F) ≈ 22.3, C(3), C(5) of C_6H_4); 116.0 (*d*, *J*(C,F) ≈ 7.4, C(2), C(6) of C_6H_4); 111.5 (CN); 86.1 (C(3)=C); 56.0 (C(1), C(5)); 36.7 (C(2), C(4)); 28.5 (C(6), C(7)). HR-MS: 267.1184 ($C_{16}H_{14}FN_3^+$; calc. 267.1172).

2.2.4. *Methyl 2-cyano-2-[8-(4-methylphenyl)-8-azabicyclo[3.2.1]octan-3-ylidene]acetate* (**2T3**) was synthesized by refluxing **2T1** (1.50 g, 6.97 mmol), methyl 2-cyanoacetate (0.77 g, 7.77 mmol), 537 mg of $AcONH_4$, and 0.12 ml of AcOH in 5 ml of toluene for 3 h in a *Dean-Stark* apparatus. The usual workup yielded an orange oil. FC (silica gel; AcOEt) yielded a yellow solid, which was further purified by FC (silica gel; CH_2Cl_2) and finally recrystallized from MeOH to give **2T3** as yellow crystalline compound. Yield: 142 mg (0.48 mol, 7%). M.p. 121–122°. IR ($CHCl_3$): 3030*w*, 3000*m*, 2955*m*, 2920*m*, 2880*w*, 2225*m*, 1725*s*, 1610*m*, 1590*s*, 1510*s*, 805*m*. ^{1}H-NMR (200 MHz, $CDCl_3$): 7.11 (*d*, $J \approx 8.5$, H–C(3), H–C(5) of C_6H_4); 6.78 (*d*, $J \approx 8.5$, H–C(2), H–C(6) of C_6H_4); 4.43 (*m*, H–C(1)); 4.36 (*m*, H–C(5)); 3.82 (*m*, H_{eq}–C(4), MeO); 2.88 (*d* with additional fine coupling, $J \approx 14$, H_{eq}–C(2)); 2.78 (*d* with additional fine coupling, $J \approx 16$, H_{ax}–C(2)); 2.58 (*d* with additional fine coupling, J ≈ 15, H_{ax}–C(4)); 2.28 (*s*, Me); 2.11 (*m*, H_{exo}–C(6), H_{exo}–C(7)); 1.73 (*m*, H_{endo}–C(6), H_{endo}–C(7)). ^{13}C-NMR (50.3 MHz, APT, $CDCl_3$): 175.5 (C(3)); 162.2 (CO); 142.7 (C(1) of C_6H_4); 130.3 (C(3), C(5) of C_6H_4); 128.0 (C(4) of C_6H_4); 115.4 (CN); 115.2 (C(2), C(6) of C_6H_4); 105.4 (C(3)=*C*); 55.6 (C(1)); 55.4 (C(5)); 52.5 (MeO); 38.0 (C(2)); 33.7 (C(4)); 28.6 (C(7)); 28.4 (C(6)); 20.3 (Me). HR-MS: 296.1481 ($C_{18}H_{20}N_2O_2^+$; calc. 296.1524).

2.2.5. *Methyl 2-cyano-2-[8-(3,5-dimethylphenyl)-8-azabicyclo[3.2.1]octan-3-ylidene]acetate* (**3T3**) was synthesized by refluxing **3T1** (1.00 g, 4.36 mmol), methyl 2-cyanoacetate (0.47 g, 4.74 mmol), 335 mg of $AcONH_4$, and 0.79 ml of AcOH in 10 ml of toluene for 2 h in a *Dean-Stark* apparatus. The usual workup yielded a dark brown solid. After several recrystallizations from AcOEt, the yellow solid isolated was finally recrystallized from hexane (with a few drops of CH_2Cl_2) to yield **3T3** as yellow crystals. Yield: 448 mg (1.44 mmol, 33%). M.p. 163–164°. IR ($CHCl_3$): 3030*m*, 3005*m*, 2855*m*, 2820*m*, 2780*w*, 2225*m*, 1725*s*, 1590*s*, 825*m*. ^{1}H-NMR (200 MHz, $CDCl_3$): 6.50 (*s*, 3 arom. H); 4.44 (*m*, H–C(1)); 4.38 (*m*, H–C(5)); 3.82 (*m*, H_{eq}–C(4), MeO); 2.90 (*d* with additional fine coupling, $J \approx 15.0$, H_{eq}–C(2)); 2.79 (*dd*, $J \approx 14.0$, 4.0, H_{ax}–C(2)); 2.60 (*dd*, $J \approx 15$, H_{ax}–C(4)); 2.29 (*s*, 2 Me); 2.08 (*m*, H_{exo}–C(6), H_{exo}–C(7)); 1.71 (*m*, H_{endo}–C(6), H_{endo}–C(7)). ^{13}C-NMR (50.3 MHz, APT, $CDCl_3$): 175.6 (C(3)); 162.2 (CO); 145.0 (C(1) of C_6H_3); 139.4 (C(3), C(5) of C_6H_3); 120.7 (C(4) of C_6H_3); 115.4 (CN); 113.0 (C(2), C(6) of C_6H_3); 105.4 (C(3)=*C*); 55.4 (C(1)); 55.1 (C(5)); 52.4 (MeO); 38.2 (C(2)); 34.0 (C(4)); 28.5 (C(7)); 28.4 (C(6)); 21.7 (Me). HR-MS: 310.1684 ($C_{19}H_{22}N_2O_2^+$; calc. 310.1682).

3. *Cambridge Structural Database Search.* The fragment defined in *QUEST* consisted of a piperidine ring with an $-CH_2CH_2-$ bridge attached on the C-atoms directly bonded to the N(1)-atom. With the exception of N(1) and C(4), the other C-atoms were restricted to have only H-atoms attached to them. *CSD* Version 5.23 (April 2002) yielded 60 refcodes (with coordinates): BENMIQ10, BRTPRN, BZOTRP, BZTRIP, BZTRMS, CANHUU, CECKUQ, CITHUI, CITJAQ, CLTRIP, CURHEC, CUVTES, CUWHOR, DAKWUH, DAKXAO, DECFAS, DECZAM, DICKUV, DUGKOF, DUMRAE, DUMRAF, DUZHEL, FEMJUC, FEMKAJ, FEMKEN, FEMKIR, FIZVUF, FIZXUH, FIZYAO, FUDHAN, GAKPAJ, GEFBOI, GOMREF, HIJDAF, HYOHBR, JATTUT, JIWMAD, JIWMEH, KOLJAW, KUDZIS, KUZSIH, KUZSON, PIMHOI, PIMHUO, PTROPN, QIRSAL, QIRSEP, QIRSIT, RACMUD, SAJWIJ, SARBIW, SECVIF, TEZTUN, TRPHDT10, TRSHYS10, VATZUL, VAVBAV, WAGGOA, YILFUU, ZEXTAX. Compounds with two non-H-substituents on the N(1)-atom were not included. The 60 refcodes represent 66 fragments. To avoid biased results, VATZUL and VAVBAV were excluded for the calculations. The central C–C bonds of the piperidine ring are in the range

1.480–1.603 Å. Averaging the central C–C bonds for each fragment result in an average value of 1.528(2) Å. For the angle C(2)–N(1)–C(6) the range is 99.8–116.6°, and the calculated average is 101.7(3)°.

REFERENCES

[1] R. Hoffmann, A. Imamura, W. J. Hehre, *J. Am. Chem. Soc.* **1968**, *90*, 1499.
[2] B. Krijnen, Ph.D. Thesis, University of Amsterdam, 1990.
[3] D. J. A. De Ridder, K. Goubitz, H. Schenk, B. Krijnen, J. W. Verhoeven, *Helv. Chim. Acta* **2003**, *86*, 799.
[4] B. Krijnen, H. B. Beverloo, J. W. Verhoeven, C. A. Reiss, K. Goubitz, D. Heijdenrijk, *J. Am. Chem. Soc.* **1989**, *111*, 4433.
[5] F. H. Allen, O. Kennard, *Chem. Des. Autom. News* **1993**, *8*, 31.
[6] H. Maag, R. Locher, J. J. Daly, I. Kompis, *Helv. Chim. Acta* **1986**, *69*, 887.
[7] A. M. Halpern, A. L. Lyons Jr., *J. Am. Chem. Soc.* **1976**, *98*, 3242.
[8] R. J. Bishop, G. Fodor, A. R. Katrizky, F. Soti, L. E. Sutton, F. J. Swinbourne, *J. Chem. Soc. C* **1966**, 74; H. W. Avdovich, G. A. Neville, *Can. J. Spectrosc.* **1983**, *28*, 1.
[9] Y. Kashman, S. Cherkez, *Tetrahedron* **1972**, *28*, 155; Y. Kashman, S. Cherkez, *Tetrahedron* **1972**, *28*, 1211.
[10] R. Hoffmann, *Acc. Chem. Res.* **1971**, *4*, 1; R. Gleiter, *Angew. Chem.* **1974**, *86*, 770; M. N. Paddon-Row, *Acc. Chem. Res.* **1982**, *15*, 245.
[11] M. Vooren, H. Schenk, C. H. MacGillavry, *Acta Crystallogr., Sect. B* **1970**, *26*, 1483; T. A. Hamor, N. Kings, *Acta Crystallogr., Sect. B* **1980**, *36*, 3153; E. Galvez, M. Martínez, G. G. Trigo, F. Florencio, J. Vilches, S. García-Blanco, *J. Mol. Struct.* **1981**, *75*, 241; J. Vilches, F. Florencio, S. García-Blanco, *Acta Crystallogr., Sect. B* **1981**, *37*, 361; J. Vilches, F. Florencio, P. Smith-Verdier, S. García-Blanco, *Cryst. Struct. Commun.* **1982**, *11*, 13.
[12] M. Ohashi, I. Morishima, K. Okada, T. Yonezawa, *J. Chem. Soc., Chem. Commun.* **1971**, 34.
[13] W. L. Duax, C. M. Weeks, D. C. Rohrer, *Top. Stereochem.* **1976**, *9*, 271.
[14] E. W. Garbisch Jr., D. H. Patterson, *J. Am. Chem. Soc.* **1963**, *85*, 3228; N. L. Allinger, M. T. Tribble, *Tetrahedron Lett.* **1971**, 3259; W. F. Bailey, H. Connon, E. L. Eliel, K. B. Wiberg, *J. Am. Chem. Soc.* **1978**, *100*, 2202; E. L. Eliel, *J. Mol. Struct.* **1985**, *126*, 385; M. E. Squillacote, J. M. Neth, *J. Am. Chem. Soc.* **1987**, *109*, 198.
[15] D. A. Dougherty, W. D. Hounshell, H. B. Schlegel, R. A. Bell, K. Mislow, *Tetrahedron Lett.* **1976**, 3479; D. A. Dougherty, H. B. Schlegel, K. Mislow, *Tetrahedron* **1978**, *34*, 1441.
[16] N. G. Rondan, M. N. Paddon-Row, P. Caramella, K. N. Houk, *J. Am. Chem. Soc.* **1981**, *103*, 2436; K. N. Houk, N. G. Rondan, F. K. Brown, W. L. Jorgensen, J. D. Madura, D. C. Spellmeyer, *J. Am. Chem. Soc.* **1983**, *105*, 5980.
[17] G. A. Jeffrey, K. N. Houk, M. N. Paddon-Row, N. G. Rondan, J. Mitra, *J. Am. Chem. Soc.* **1985**, *107*, 321.
[18] W. H. Watson, J. Galloy, D. A. Grossie, P. D. Bartlett, G. L. Combs Jr., *Acta Crystallogr., Sect. C* **1984**, *40*, 1050; L. A. Paquette, G. DeLucca, K. Ohkata, J. C. Gallucci, *J. Am. Chem. Soc.* **1985**, *107*, 1015; A. A. Pinkerton, D. Schwarzenbach, J.-L. Birbaum, P.-A. Carrupt, L. Schwager, P. Vogel, *Helv. Chim. Acta* **1984**, *67*, 1136.
[19] R. Gleiter, L. A. Paquette, *Acc. Chem. Res.* **1983**, *16*, 328; R. Gleiter, *Pure Appl. Chem.* **1987**, *59*, 1585.
[20] R. de Gelder, R. A. G. de Graaff, H. Schenk, *Acta Crystallogr., Sect. A* **1993**, *49*, 287.
[21] 'XTAL3.7 System', Eds. S. R. Hall, D. J. du Boulay, R. Olthof-Hazekamp, University of Western Australia, Lamb, Perth, Australia, 2000.
[22] W. H. Zachariasen, *Acta Crystallogr.* **1967**, *23*, 558.
[23] A. L. Spek, *Acta Crystallogr., Sect. A* **1990**, *46*, C-34.
[24] G. Jones, in 'Organic Reactions', Eds. R. Adams, A. H. Blatt, V. Boekelheide, T. L. Cairns, A. C. Cope, D. J. Cram, H. O. House, J. Wiley & Sons Inc., New York, 1967, Vol. 15, Chapt. 2, p. 204.
[25] N. Elming, in 'Advances in Organic Chemistry. Methods and Results', Eds. R. A. Raphael, E. C. Taylor, H. Wynberg, Interscience Publishers Inc., New York, 1960, Vol. II, p. 67–115 and ref. cit. therein; F. M. Menger, D. J. Goldsmith, L. Mandell, 'Organic Chemistry, a Concise Approach', 2nd edition, W. A. Benjamin Inc., California, 1975, p. 334.
[26] S. Archer, U.S. Pat. 2.798.874 to Sterling Drug, Inc., 1957, example 22.
[27] T. Sato, K. Sato, T. Mukai, *Bull. Chem. Soc. Jpn.* **1971**, *44*, 1708.

Received August 22, 2002